Editors' Suggestion | Featured in Physics

Disorder-Enhanced and Disorder-Independent Transport with Long-Range Hopping: Application to Molecular Chains in Optical Cavities

Nahum C. Chávez,[1,2] Francesco Mattiotti,[1,3,4] J. A. Méndez-Bermúdez,[2] Fausto Borgonovi,[1,5] and G. Luca Celardo[2]

[1]*Dipartimento di Matematica e Fisica and Interdisciplinary Laboratories for Advanced Materials Physics, Università Cattolica, via Musei 41, 25121 Brescia, Italy*

[2]*Benemérita Universidad Autónoma de Puebla, Apartado Postal J-48, Instituto de Física, 72570, Mexico*

[3]*Istituto Nazionale di Fisica Nucleare, Sezione di Pavia, via Bassi 6, I-27100, Pavia, Italy*

[4]*Department of Physics, University of Notre Dame, Notre Dame, Indiana 46556, USA*

[5]*Istituto Nazionale di Fisica Nucleare, Sezione di Milano, via Celoria 16, I-20133, Milano, Italy*

(Received 14 October 2020; accepted 2 February 2021; published 12 April 2021)

Overcoming the detrimental effect of disorder at the nanoscale is very hard since disorder induces localization and an exponential suppression of transport efficiency. Here we unveil novel and robust quantum transport regimes achievable in nanosystems by exploiting long-range hopping. We demonstrate that in a 1D disordered nanostructure in the presence of long-range hopping, transport efficiency, after decreasing exponentially with disorder at first, is then enhanced by disorder [disorder-enhanced transport (DET) regime] until, counterintuitively, it reaches a disorder-independent transport (DIT) regime, persisting over several orders of disorder magnitude in realistic systems. To enlighten the relevance of our results, we demonstrate that an ensemble of emitters in a cavity can be described by an effective long-range Hamiltonian. The specific case of a disordered molecular wire placed in an optical cavity is discussed, showing that the DIT and DET regimes can be reached with state-of-the-art experimental setups.

DOI: 10.1103/PhysRevLett.126.153201

Introduction.—Achieving high efficiency for energy or charge transport in quantum wires is fundamental for quantum technologies related to quantum computation and basic energy science [1–11]. One of the main challenges is to control the detrimental effects of noise and disorder which naturally occur in realistic situations. It is well known that disorder induces localization [12,13] and exponential suppression of transport in typical 1D nanostructures. One of the most ambitious goals in quantum transport is to achieve dissipationless quantum wires, able to transport energy or charge without suffering the detrimental effects of disorder and/or noise.

Here, to overcome disorder suppression of transport, we propose to exploit long-range interactions. Long-range interactions can arise due to microscopic interactions or by engineering the coupling to external degrees of freedom. They have been recently emulated in ion traps [14] and are relevant in several realistic systems such as cold atomic clouds [15] and excitonic transport in molecular aggregates [16–18]. Long-range interactions present many contradictory features [19–21]. Specifically, the interplay of localization and long-range interactions is widely debated in literature [19,20,22–28]. Indeed, contrary to the common lore that long range should destroy Anderson localization [29,30], strong signatures of localization have been reported recently in long-range interacting systems [19,22,23], thus questioning their utility in achieving efficient transport. Here we demonstrate that localized states in long-range interacting systems have a hybrid character, with an exponentially localized peak and extended tail, which allows these states to support robust quantum transport.

Among the most important features of long-range systems, there is the emergence of a gapped ground state [19,31]. In the gapped regime, while the ground state is extended and robust to disorder, the excited states present a hybrid nature with an exponentially localized peak superimposed to an extended tail [19,32,33]. While being very relevant to transport, since they constitute the vast majority of the states, due to their hybrid nature it is not clear what kind of transport they will be able to support. By using different standard figures of merit of transport efficiency, we unveil several regimes directly determined by the hybrid nature of the excited states. Specifically, we develop a new method to compute the stationary current, based on an effective non-Hermitian Hamiltonian formalism, which is equivalent to a Lindblad master equation and it is much more efficient. We demonstrate, in the presence of long-range hopping, the emergence of extremely robust transport regimes arising as the disorder strength is increased: a disorder-enhanced transport (DET) regime and, at larger disorder strength, a disorder-independent transport (DIT) regime, where transport efficiency is independent of disorder over several orders of magnitude of disorder strength. The latter regime persists until disorder is so large to close

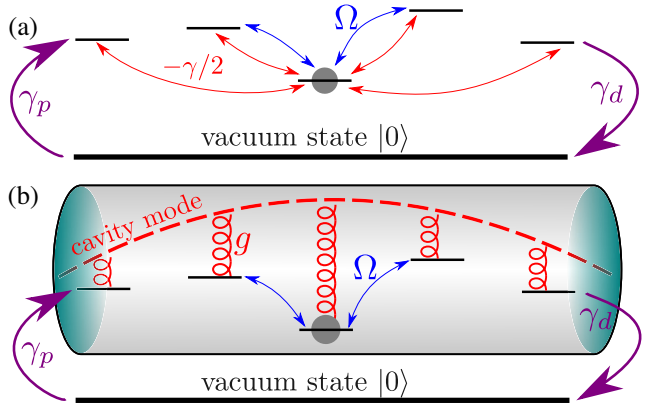

FIG. 1. (a),(b) Two different setups for a disordered chain with excitation pumping γ_p at one edge of the chain and draining γ_d at the opposite edge. Here, Ω is the hopping between nearest-neighbor sites. The arrows indicate the hopping paths available for an excitation (gray circle) present at the center of the chain. The energy of the sites is disordered. (a) A long-range coupling $-\gamma/2$ is present between each pair of sites. (b) The chain is placed inside an optical cavity, where g is the coupling of each site to the cavity mode.

the energy gap. We can explain the origin of this interesting behavior by considering that in the presence of an energy gap, disorder will mix the excited states, while leaving the ground state fully extended. The presence of an extended ground state imposes an orthogonality condition on the excited states which prevents their full single-site localization and generates an extended tail able to support robust transport over the whole energy spectrum.

In order to highlight the relevance of our findings, we analyze realistic setups consisting of an ensemble of emitters inside a cavity, focusing on the case of molecular chains in optical cavities. Recently these systems have been studied experimentally [9] and analyzed theoretically [2,3,34]. Here we show that, in the strong coupling regime [35,36], the cavity induces an effective long-range hopping between the emitters, allowing us to test our findings of both DET and DIT regimes in state-of-the-art experimental setups.

Model.—As a paradigmatic model of a disordered chain in the presence of long-range hopping, we analyze the 1D Anderson model [12] with all-to-all hopping [19], see Fig. 1(a),

$$H = H_0 + V \quad \text{with} \quad V = -\frac{\gamma}{2}\sum_{i\neq j}|i\rangle\langle j|, \tag{1}$$

where $|j\rangle$ is the site basis and γ is the strength of the distance-independent long-range hopping. H_0 describes the Anderson model where a particle hops between neighbor sites of a linear chain in the presence of on-site disorder,

$$H_0 = \sum_{j=1}^{N}\epsilon_j|j\rangle\langle j| + \Omega\sum_{j=1}^{N-1}(|j\rangle\langle j+1| + |j+1\rangle\langle j|), \tag{2}$$

where ϵ_i are random energies uniformly distributed in $[-W/2, W/2]$, where W is the disorder strength and Ω is the tunneling transition amplitude between nearest neighbor sites.

The eigenstates of the Anderson Model ($\gamma = 0$) are localized exponentially, $\psi_n \sim \exp(-|n-n_0|/\xi)$, where $\xi \approx 105.2(\Omega/W)^2$ is the localization length in the middle of the energy band. This implies that the transmission always decays exponentially with the disorder strength as $\approx \exp(-N/\xi)$ [37,38].

In the presence of long-range hopping ($\gamma \neq 0$), and in the absence of disorder ($W = 0$), the emergence of an energy gap $\Delta = N\gamma/2$ has been found in Refs. [19,31]. Indeed, the long-range hopping induces the fully symmetric ground state to be gapped from the other excited states. Disorder will destroy the energy gap above the disorder threshold [31] [for details, see the Supplementary Material (SM) [39]],

$$W_{\text{gap}} = \frac{\gamma}{2}N\ln N. \tag{3}$$

In order to understand how transport properties are affected by long-range hopping, we analyze several figures of merit of transport efficiency, focusing on the stationary current widely used in literature [2,3,34]. Pumping and draining are introduced at the chain edges, see Fig. 1(a), and the dynamics is described by the Lindblad master equation [43]:

$$\frac{d\rho}{dt} = -\frac{i}{\hbar}[H,\rho] + \sum_{\eta=p,d}\mathcal{L}_\eta[\rho], \tag{4}$$

where $\mathcal{L}_\eta[\rho] = -\{L_\eta^\dagger L_\eta, \rho\} + 2L_\eta\rho L_\eta^\dagger$ are two dissipators inducing pumping on the first site [$L_p = \sqrt{\gamma_p/(2\hbar)}|1\rangle\langle 0|$] and draining from the last site [$L_d = \sqrt{\gamma_d/(2\hbar)}|0\rangle\langle N|$], respectively ($|0\rangle$ is the vacuum state). From the steady-state solution of Eq. (4) one can find the stationary current,

$$I = \frac{\gamma_d}{\hbar}\langle N|\rho_{\text{SS}}|N\rangle, \tag{5}$$

where ρ_{SS} is the steady-state density operator. Since the master equation approach is numerically very expensive, we use a definition of current based on a non-Hermitian Schrödinger equation, computationally less expensive. The results obtained with this approach are identical to the master equation method, as we prove analytically in Sec. V. B of the SM [39]. To define the current, we compute the average time needed to leave the 1D chain if the excitation is initially on the first site $|1\rangle$ and a drain is present on the last site $|N\rangle$. The average transfer time is defined as [44–47]

$$\tau = \frac{\gamma_d}{\hbar}\int_0^\infty t|\Psi_N(t)|^2 dt, \tag{6}$$

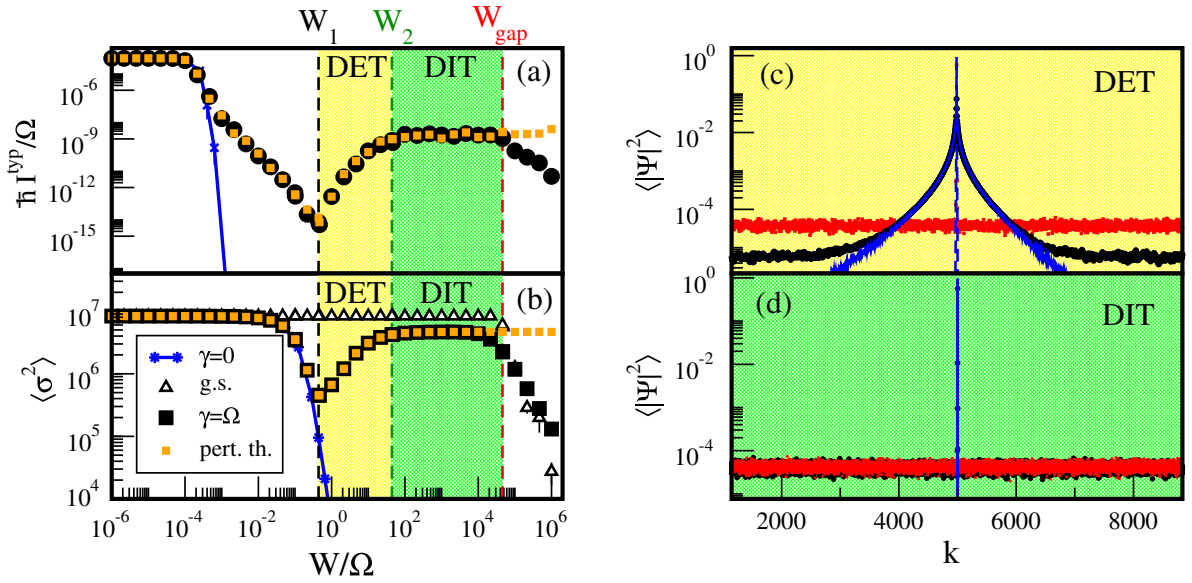

FIG. 2. (a) Normalized typical current $\hbar I^{\mathrm{typ}}/\Omega$ versus the normalized static disorder W/Ω. (b) Average variance $\langle\sigma^2\rangle$ versus the normalized static disorder W/Ω for the ground state (triangles) and the excited states (all other sets). The blue curves show the case $\gamma = 0$, the orange squares the perturbative approach (details are given in the SM [39]). Dashed vertical lines indicate the different critical disorders given by Eqs. (3), (10), and (11). (c),(d) Average shape of the eigenfunctions (details concerning the process of averaging are given in SM [39]), $\langle|\Psi|^2\rangle$ versus the site basis k. Different disorder regimes are shown. (c) (DET) $W_1 \leq W \leq W_2$, $W/\Omega = 1$ (black) and $W/\Omega = 44.02$ (red); (d) (DIT) $W_2 < W < W_{\mathrm{gap}}$, $W/\Omega = 10^2$ (black) and $W/\Omega = 10^3$ (red). Here, $N = 10^4$, $\gamma_p = \gamma_d = \gamma = \Omega$, and $N_r = 100$ disorder configurations. In (c),(d) symbols are compared with blue curves indicating the case $\gamma = 0$.

where $\Psi_N(t)$ is the probability amplitude on the drain site at time t, evolved under the effective Hamiltonian H_{eff} [48,49],

$$(H_{\mathrm{eff}})_{k,l} = (H)_{k,l} - i\frac{\gamma_d}{2}\delta_{k,N}\delta_{l,N}, \tag{7}$$

with H given in Eq. (1) and the non-Hermitian term representing the drain. A rate equation can be derived, by assigning a drain frequency $1/\tau$ and a pumping frequency $\gamma_p/\hbar$, connecting the chain population P_e to the vacuum state $|0\rangle$ with population P_0:

$$\frac{dP_0}{dt} = -\frac{\gamma_p}{\hbar}P_0 + \frac{1}{\tau}P_e, \qquad P_0 + P_e = 1. \tag{8}$$

From the steady-state populations $P_e^{\mathrm{SS}} = \gamma_p/(\gamma_p + \hbar/\tau)$ we obtain the current $I = P_e^{\mathrm{SS}}/\tau$ and its typical value,

$$I^{\mathrm{typ}} = e^{\langle \ln I\rangle} \quad \text{with} \quad \langle \ln I\rangle \equiv \left\langle \ln\left(\frac{1}{\tau}\frac{\gamma_p}{\gamma_p + \frac{\hbar}{\tau}}\right)\right\rangle, \tag{9}$$

where $\langle\cdots\rangle$ represents the average over disorder configurations.

Another important figure of merit for the transport is the average variance $\langle\sigma^2\rangle$ of the excited states $|\alpha\rangle$, defined as $\sigma^2 = [1/(N-1)]\sum_{\alpha=1}^{N-1}\sigma_\alpha^2$, where $\sigma_\alpha^2 \equiv \langle\alpha|x^2|\alpha\rangle - \langle\alpha|x|\alpha\rangle^2$. This can be related to the stationary variance obtained from the dynamical spreading of a wave packet initially localized at the center of the chain; see SM [39]. Moreover, in the SM [39], we also considered another figure of merit for transport, i.e., the integrated transmission. Transport properties revealed by the three different figures of merit are qualitatively the same.

Results for long-range systems.—In Figs. 2(a) and 2(b), $\hbar I^{\mathrm{typ}}/\Omega$, see Eq. (9), and $\langle\sigma^2\rangle$ are shown as a function of the normalized disorder strength W/Ω for a chain with $N = 10^4$ sites. For small disorder both quantities decrease with W exponentially, similarly to the Anderson model ($\gamma = 0$, blue curves). Counterintuitively, by increasing W, the transport efficiency at first increases (DET regime), until it reaches a plateau, where the dependence on the disorder strength is extremely weak for several orders of magnitude of W (DIT regime). The latter persists approximately up to W_{gap}.

Since the variance $\langle\sigma^2\rangle$ of the excited eigenstates, Fig. 2(b), closely follows the behavior of the typical current I^{typ}, Fig. 2(a), we can try to understand the different transport regimes analyzing the average shape of the eigenfunctions $\langle|\Psi|^2\rangle$ of the excited states as a function of the site basis k for different disorder strengths W.

Specifically, in the presence of long-range hopping [19,32,33], in the gapped regime, the excited states have a hybrid nature, with an exponentially localized peak, identical to the Anderson model peak, and extended flat tails, see Figs. 2(c) and 2(d), where the average shape of the eigenfunctions $\langle|\Psi|^2\rangle$ in the DET and DIT regimes are shown. Note that, while in the DET regime the tails increase

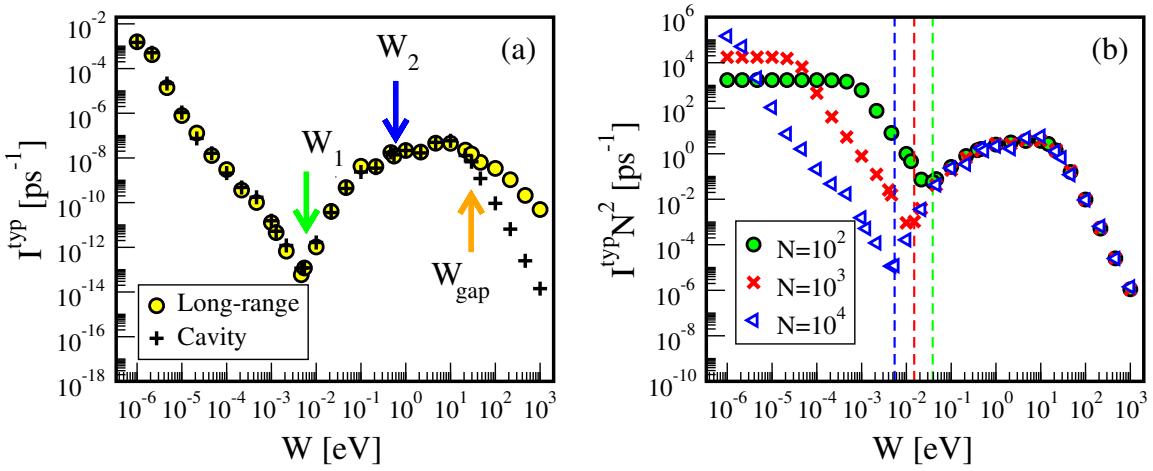

FIG. 3. (a) Typical current I^{typ}, Eq. (9), versus the static disorder W. The results for a linear chain in an optical cavity Eq. (12) (crosses) are compared with a long-range hopping model Eq. (1) (circles). Parameters for the linear chain in an optical cavity are $N = 10^4$, $\Omega = 0.0124$ eV, $\hbar\omega_c = 2$ eV, $\mu \approx 36$ D, $g_c = 3.188$ eV, $\gamma_p = \gamma_d = 0.0124$ eV. The long-range hopping model has been obtained using the same Ω value and setting $\gamma = 2g_c/N$ in Eq. (1). The number of disorder configurations N_r is such that $N_r \times N = 10^6$. (b) Normalized typical current $I^{\mathrm{typ}}N^2$ versus the static disorder W for a linear chain in an optical cavity for different N values, as indicated in the legend. Vertical dashed lines represent the values of W_1 for different system sizes. Other parameters are the same as in (a).

with the disorder strength W, they are independent of it in the DIT regime. Hybrid shapes of the eigenfuctions have been reported in other long-range interacting systems [32,50].

An analytical expression for the disorder thresholds, separating the different transport regimes, can be found as follows. When the probability of the exponentially localized peak at the chain edges, $\approx \exp(-N/2\xi)$, becomes equal to the average probability in the tails (which scales as $1/N$; see SM [39]), we have $\exp(-N/2\xi) \approx 1/N$. Recalling that $\xi \approx 105.2(\Omega/W)^2$, we get the disorder threshold W_1:

$$W_1 \approx \sqrt{\frac{210.4 \ln N}{N}}\Omega. \tag{10}$$

For $W > W_1$, the amplitude of the extended tails increases with the disorder strength W, see Fig. 2(c), until the eigenfunction tails become independent of W; see Fig. 2(d). The disorder threshold W_2 above which this happens can be obtained by imposing that the probability on the closest sites to the peak is equal to the probability in the tails, $\exp(-1/2\xi) = 1/N$, so that

$$W_2 \approx \sqrt{210.4 \ln N}\Omega. \tag{11}$$

The validity of the predicted scaling of the different transport regimes with N and γ is discussed below and also in the SM [39].

One might think that these interesting transport regimes originate from the coupling induced by disorder between the unperturbed excited states and the extended unperturbed ground state. Even if this coupling exists, it is not the main reason for the DET and DIT regimes. Indeed, a semianalytical perturbative expression for the eigenstates in the gapped regime allows us to compute all the relevant observables, see orange dots in Figs. 2(a) and 2(b), completely neglecting the coupling mediated by disorder between the unperturbed excited states and the extended unperturbed ground state; see details in SM [39]. This indicates that the DET and DIT regimes have their origin in the existence of an extended ground state which, by imposing an orthogonality condition on all the excited states, generates their extended tails.

Applications to molecular chains in optical cavities.—Here we show that a chain of emitters in a cavity [2,3,34] can be described in terms of an effective long-range hopping model arising from the coupling of the emitters with the cavity mode. This implies that our results are relevant for a vast variety of other systems such as Rydberg atoms, polar molecules, and molecular chains [3].

In the following we focus on the case in which the emitters are molecules. This is particularly interesting due to the large coupling (comparable with k_BT with $T = 300$ K) between the molecules. Nevertheless, the same discussion can be applied to any other kind of emitters. For a molecular chain, at resonance with a cavity mode [3,34] the Hamiltonian is given by

$$H_{\mathrm{cav}} = H_0 + g\sum_{j=1}^{N}(|j\rangle\langle c| + |c\rangle\langle j|), \tag{12}$$

where H_0 is defined in Eq. (2) and $|c\rangle$ represents a single excitation in the cavity mode (with no excitation in the

chain). The coupling g of the emitters with the resonant optical mode is given by [51]

$$g = \sqrt{\frac{2\pi\mu^2\hbar\omega_c}{V_c}}, \tag{13}$$

where μ is the molecular transition dipole, ω_c is the cavity mode frequency, and V_c is the cavity mode volume.

Since the coupling to the cavity mode is the same for all molecules, it is possible to show [2,3] that only the fully symmetric state $|d\rangle$ in the chain is coupled to the cavity mode with a collective coupling strength $g_c = \sqrt{N}g$. This coupling induces two polaritonic states, $|p_\pm\rangle = 1/\sqrt{2}(|d\rangle \pm |c\rangle)$, with an energy splitting of $2g_c$, while the other $N-1$ states with a bandwidth 4Ω, in the absence of disorder, are decoupled from the cavity mode. In the strong coupling regime, $g_c \gg \Omega$, one of the polaritonic states will become the ground state of the system and it will be gapped from the excited states by an energy $\approx g_c$. By imposing

$$N\gamma_{\text{eff}}/2 = g_c, \tag{14}$$

we determine the effective long-range coupling γ_{eff} which would produce the same energy gap in the absence of disorder; see SM [39] for details.

Since the coupling g is inversely proportional to V_c, see Eq. (13), which typically scales like N, in the following we consider a fixed collective coupling $g_c = \sqrt{N}g \approx 3.2$ eV [36,52], which corresponds to a cavity mode volume $V_c = 10^4$ nm^3 [53] for a molecular chain of $N = 10^4$ with $\mu \approx 36$ D [9].

In Fig. 3(a) we plot the typical current I^{typ} versus the disorder strength W for a chain of 10^4 molecules in an optical cavity (crosses). Interestingly, this current is reproduced extremely well by the current obtained with the effective long-range coupling Eq. (14) (circles) for $W < W_{\text{gap}}$. For $W > W_{\text{gap}}$ both polaritonic states mix with all the other states and the differences between the long-range model and the chain in the cavity model emerge. In Fig. 3(b) the typical (normalized) current $I^{\text{typ}}N^2$ for the cavity model, Eq. (12), is shown for different chain sizes N. Note that $I^{\text{typ}} \propto 1/N^2$ for $W > W_1$, instead of decreasing exponentially with N, as for the localized regime in the absence of long-range hopping.

Conclusions.—Controlling the detrimental effects of disorder at the nanoscale is one of the main challenges in achieving efficient energy transport. Here we have shown that long-range hopping can lead to a disorder-enhanced and a disorder-independent transport regime, extending over several orders of magnitude of disorder strength. Our results could be tested in several systems where long-range hopping is present, such as molecular aggregates [48], ion traps [14], and cold atomic clouds [15]. Remarkably, we have also shown that a system of emitters coupled to a cavity mode can be mapped to a long-range hopping system. This makes our results applicable to a vast variety of other physical systems, such as molecular chains in optical cavities, Rydberg atoms, and polar molecules [3]; see SM [39] for realistic parameters. Typically, for molecular chains in optical cavities $\Omega \approx 0.03$ eV, $N \approx 10^5$, and $g_c \approx 1$ eV [3], so that $W_1 \approx 5 \times 10^{-3}$ eV, $W_2 \approx 1.5$ eV, and $W_{\text{gap}} \approx g_c \ln N \approx 11.5$ eV. Since natural disorder typically ranges from 1 to 10 Ω, we can easily reach the DET regime, with currents in the measurable range of tens of nanoampere [9]. In other experimental setups, such as ion traps, the spreading of an initially localized excitation in the middle of the chain would provide the best way to access both the DET and DIT regime. Indeed, the stationary variance of the excitation, obtained from the spreading of a localized wave packet, is well described by the average variance of the eigenstates shown in Fig. 2(b); see SM [39] for details. In perspective, it would be interesting to analyze the effect of thermal noise on transport in long-range systems.

We acknowledge useful discussions with Thomas Botzung, Jérôme Dubail, Robin Kaiser, David Hagenmüller, Guido Pupillo, Johannes Schachenmayer, and Stefan Schütz. F. B. and F. M. acknowledge support by the Iniziativa Specifica INFN-DynSysMath. This work has been financially supported by the Catholic University of Sacred Heart within the program of promotion and diffusion of scientific research. Research has also been financially supported by Ministero dell'Istruzione, dell'Università e della Ricerca within the Project No. PRIN 20172H2SC4. G. L. C. acknowledges the funding of CONACyT Ciencia Basica Project No. A1-S-22706.

[1] D. M. Coles, N. Somaschi, P. Michetti, C. Clark, P. G. Lagoudakis, P. G. Savvidis, and D. G. Lidzey, Nat. Mater. **13**, 712 (2014).
[2] J. Feist and F. J. Garcia-Vidal, Phys. Rev. Lett. **114**, 196402 (2015).
[3] J. Schachenmayer, C. Genes, E. Tignone, and G. Pupillo, Phys. Rev. Lett. **114**, 196403 (2015).
[4] X. Zhong, T. Chervy, L. Zhang, A. Thomas, J. George, C. Genet, J. A. Hutchison, and T. W. Ebbesen, Angew. Chem. Int. Ed. **56**, 9034 (2017).
[5] G. Lerario, D. Ballarini, A. Fieramosca, A. Cannavale, A. Genco, F. Mangione, S. Gambino, L. Dominici, M. De Giorgi, G. Gigli *et al.*, Light Sci. Appl. **6**, e16212 (2017).
[6] M. Reitz, F. Mineo, and C. Genes, Sci. Rep. **8**, 9050 (2018).
[7] M. Du, L. A. Martínez-Martínez, R. F. Ribeiro, Z. Hu, V. M. Menon, and J. Yuen-Zhou, Chem. Sci. **9**, 6659 (2018).
[8] C. Schäfer, M. Ruggenthaler, H. Appel, and A. Rubio, Proc. Natl. Acad. Sci. U.S.A. **116**, 4883 (2019).
[9] E. Orgiu, J. George, J. Hutchison, E. Devaux, J. Dayen, B. Doudin, F. Stellacci, C. Genet, J. Schachenmayer, C. Genes, G. Pupillo, P. Samorì, and T. W. Ebbesen, Nat. Mater. **14**, 1123 (2015).

[10] D. Hagenmüller, J. Schachenmayer, S. Schütz, C. Genes, and G. Pupillo, Phys. Rev. Lett. **119**, 223601 (2017).
[11] D. Hagenmüller, S. Schütz, J. Schachenmayer, C. Genes, and G. Pupillo, Phys. Rev. B **97**, 205303 (2018).
[12] P. W. Anderson, Phys. Rev. **109**, 1492 (1958).
[13] E. Abrahams, *50 Years of Anderson Localization* (World Scientific, Singapore, 2010).
[14] P. Jurcevic, B. P. Lanyon, P. Hauke, C. Hempel, P. Zoller, R. Blatt, and C. F. Roos, Nature (London) **511**, 202 (2014).
[15] W. Guerin, M. Rouabah, and R. Kaiser, J. Mod. Opt. **64**, 895 (2017).
[16] J. Strümpfer, M. Sener, and K. Schulten, J. Phys. Chem. Lett. **3**, 536 (2012).
[17] M. Gullì, A. Valzelli, F. Mattiotti, M. Angeli, F. Borgonovi, and G. L. Celardo, New J. Phys. **21**, 013019 (2019).
[18] F. C. Spano, J. R. Kuklinski, and S. Mukamel, J. Chem. Phys. **94**, 7534 (1991).
[19] G. L. Celardo, R. Kaiser, and F. Borgonovi, Phys. Rev. B **94**, 144206 (2016).
[20] L. F. Santos, F. Borgonovi, and G. L. Celardo, Phys. Rev. Lett. **116**, 250402 (2016).
[21] D.-M. Storch, M. Van den Worm, and M. Kastner, New J. Phys. **17**, 063021 (2015).
[22] X. Deng, V. E. Kravtsov, G. V. Shlyapnikov, and L. Santos, Phys. Rev. Lett. **120**, 110602 (2018).
[23] P. A. Nosov, I. M. Khaymovich, and V. E. Kravtsov, Phys. Rev. B **99**, 104203 (2019).
[24] P. A. Nosov and I. M. Khaymovich, Phys. Rev. B **99**, 224208 (2019).
[25] F. A. B. F. de Moura, A. V. Malyshev, M. L. Lyra, V. A. Malyshev, and F. Domínguez-Adame, Phys. Rev. B **71**, 174203 (2005).
[26] F. Liu, R. Lundgren, P. Titum, G. Pagano, J. Zhang, C. Monroe, and A. V. Gorshkov, Phys. Rev. Lett. **122**, 150601 (2019).
[27] A. Lerose, B. Žunkovič, A. Silva, and A. Gambassi, Phys. Rev. B **99**, 121112(R) (2019).
[28] T. Mori, J. Phys. A **52**, 054001 (2019).
[29] L. S. Levitov, Europhys. Lett. **9**, 83 (1989).
[30] F. Evers and A. D. Mirlin, Rev. Mod. Phys. **80**, 1355 (2008).
[31] N. C. Chávez, F. Mattiotti, J. A. Méndez-Bermúdez, F. Borgonovi, and G. L. Celardo, Eur. Phys. J. B **92**, 144 (2019).
[32] G. Celardo, A. Biella, L. Kaplan, and F. Borgonovi, Fortschr. Phys. **61**, 250 (2013).
[33] A. Biella, F. Borgonovi, R. Kaiser, and G. L. Celardo, Europhys. Lett. **103**, 57009 (2013).
[34] T. Botzung, D. Hagenmüller, S. Schütz, J. Dubail, G. Pupillo, and J. Schachenmayer, Phys. Rev. B **102**, 144202 (2020).
[35] V. M. Agranovich, M. Litinskaia, and D. G. Lidzey, Phys. Rev. B **67**, 085311 (2003).
[36] S. Kéna-Cohen, S. A. Maier, and D. D. Bradley, Adv. Opt. Mater. **1**, 827 (2013).
[37] D. J. Thouless, in *Ill-Condensed Matter*, edited by R. Balian, R. Maynard, and G. Toulouse (North-Holland, Amsterdam, 1979).
[38] F. M. Izrailev, S. Ruffo, and L. Tessieri, J. Phys. A **31**, 5263 (1998).
[39] See Supplemental Material http://link.aps.org/supplemental/10.1103/PhysRevLett.126.153201 for detailed calculations and supplemental results, including Refs. [40–42].
[40] G. L. Celardo and L. Kaplan, Phys. Rev. B **79**, 155108 (2009).
[41] S. Datta, *Quantum Transport: Atom to Transistor* (Cambridge University Press, Cambridge, England, 2005).
[42] V. V. Sokolov, I. Rotter, D. V. Savin, and M. Müller, Phys. Rev. C **56**, 1031 (1997).
[43] H.-P. Breuer and F. Petruccione, *The Theory of Open Quantum Systems* (Oxford University Press, New York, 2002).
[44] C. M. Kropf, A. Valli, P. Franceschini, G. L. Celardo, M. Capone, C. Giannetti, and F. Borgonovi, Phys. Rev. B **100**, 035126 (2019).
[45] C. M. Kropf, G. L. Celardo, C. Giannetti, and F. Borgonovi, Physica E Low Dimens. Syst. Nanostruct. **120**, 114023 (2020).
[46] M. Mohseni, P. Rebentrost, S. Lloyd, and A. Aspuru-Guzik, J. Chem. Phys. **129**, 174106 (2008).
[47] P. Rebentrost, M. Mohseni, I. Kassal, S. Lloyd, and A. Aspuru-Guzik, New J. Phys. **11**, 033003 (2009).
[48] G. L. Celardo, F. Borgonovi, M. Merkli, V. I. Tsifrinovich, and G. P. Berman, J. Phys. Chem. C **116**, 22105 (2012).
[49] Y. Zhang, G. L. Celardo, F. Borgonovi, and L. Kaplan, Phys. Rev. E **95**, 022122 (2017).
[50] T. Botzung, D. Vodola, P. Naldesi, M. Müller, E. Ercolessi, and G. Pupillo, Phys. Rev. B **100**, 155136 (2019).
[51] M. O. Scully and M. S. Zubairy, *Quantum Optics* (Cambridge University Press, Cambridge, England, 1997).
[52] S. Gambino, M. Mazzeo, A. Genco, O. Di Stefano, S. Savasta, S. Patanè, D. Ballarini, F. Mangione, G. Lerario, D. Sanvitto, and G. Gigli, ACS Photonics **1**, 1042 (2014).
[53] K. J. Vahala, Nature (London) **424**, 839 (2003).